Cosmological Constraints and Bayesian Evidence for Coupled ϕCDM with DESI DR2 Observations

S. D. Pathak[1†] Sahit Kumar[2‡] Anil Kandel[3§] Jyoti Wadhwa[4¶]

[1]Amity School of Applied Sciences, Amity University Uttar Pradesh, Lucknow Campus, 226028, Lucknow, India
[2]School of Physics, Shri Mata Vaishno Devi University, Katra -182320, India
[3]Department of Physics, St.Xavier's College, Tribhuvan University, Kathmandu, Nepal
[4]School of Chemical Engineering and Physical Sciences, Lovely Professional University, Phagwara, Punjab, 144411, India

Abstract: We investigate a coupled ϕCDM cosmological model in which energy exchange between dark energy and dark matter is governed by the derivative interaction term $Q = 3\alpha\dot{\rho}_m$. We constrain the model using baryon acoustic oscillation measurements from DESI Data Release 2, combined with compressed CMB likelihoods and Type Ia supernova datasets, including Pantheon$^+$, DES-Dovekie, and Union3. Parameter estimation is performed using Markov Chain Monte Carlo methods, and Bayesian evidence is used to compare the model with ΛCDM. We find that the interaction parameter α is tightly constrained at the $O(10^{-4})$ level and remains consistent with zero within 1σ across all dataset combinations, indicating no statistically significant evidence for dark sector interactions. The dark energy equation-of-state parameter remains close to $w_\phi = -1$, with only mild, statistically insignificant deviations toward a quintessence-like regime. Although the inferred Hubble parameter shifts slightly toward higher values relative to ΛCDM, this shift is insufficient to resolve the H_0 tension. The matter density parameter is consistent between the two models within uncertainties. Bayesian model comparison consistently favors ΛCDM, with evidence ranging from moderate to strong depending on the dataset combination. Overall, in light of current observations, the coupled ϕCDM model does not provide a significant improvement over the standard cosmological scenario.

Keywords: interacting dark energy, bayesian model comparison, DESI DR2 constraints

DOI: 10.1088/1674-1137/aeb3f0 **CSTR:**

CPC Accepted

I. INTRODUCTION

Independent cosmological observations [1−5] indicate that the Universe is undergoing accelerated expansion, commonly attributed to dark energy [6, 7]. Dark energy constitutes about 70% of the total energy density and is well described within the ΛCDM framework. Although dark energy dominates the current dynamics of the Universe, its fundamental origin and physical properties remain unknown, posing one of the most significant unresolved questions in contemporary cosmology. The cosmological constant provides a phenomenologically consistent explanation that agrees with a broad range of observational probes; however, it is accompanied by serious theoretical concerns, particularly the well-known cosmological constant problem [8, 9]. This framework also faces the cosmic coincidence problem [10], namely the puzzling question of why the dark energy density is of the same order of magnitude as the matter density precisely in the present epoch.

In addition to this long-standing puzzle, a recent tension has emerged in cosmology, suggesting a possible time-varying dark energy component. In particular, analyses of baryon acoustic oscillation (BAO) measurements from DESI 2024, combined with Type Ia supernova (SNe Ia) data, indicate a preference for dynamical dark energy over a cosmological constant at the 2.5–3.9σ level [11]. Incorporating the latest DESI Data Release 2 into a joint BAO and SNe Ia analysis further strengthens this preference, raising the statistical significance beyond 4σ [12−14]. Collectively, these findings point toward a possible deviation from a strictly constant dark-energy sector, thereby motivating the investigation of cosmological models beyond the standard ΛCDM paradigm. In the context of DESI DR2, several recent studies further support this behavior, as discussed in [15−28].

These cosmological challenges have prompted extensive investigations of alternative scenarios, including

Received 21 April 2026; Accepted 13 October 2026; Accepted manuscript online 22 September 2026

† E-mail: sdpathak@lko.amity.edu
‡ E-mail: sahit.kumar@smvdu.ac.in
§ E-mail: anil.kandel3227@gmail.com
¶ E-mail: jyotiwadhwa16@gmail.com

©2026 Chinese Physical Society and the Institute of High Energy Physics of the Chinese Academy of Sciences and the Institute of Modern Physics of the Chinese Academy of Sciences and IOP Publishing Ltd. All rights, including for text and data mining, AI training, and similar technologies, are reserved.

evolving dark energy models and modifications of gravitational theory on cosmological scales. In dynamical dark energy frameworks, the equation-of-state parameter is treated as a time-dependent quantity rather than a fixed constant. This departure from the cosmological constant hypothesis allows for richer phenomenology in the late-time expansion history. Scalar field realizations constitute a major class within this category, including quintessence [29−33], phantom [34], tachyon [35, 36], and quintom models [37]. In these scenarios, cosmic acceleration emerges from the evolution of an effective scalar degree of freedom whose dynamics determine the background expansion rate. An alternative conceptual route attributes the observed cosmic acceleration to modifications of the gravitational sector itself. Rather than invoking an additional dark energy component, modified gravity theories extend the geometric part of the field equations. In this context, $f(R)$ gravity [38, 39] generalizes the Einstein–Hilbert action by replacing the Ricci scalar R with an arbitrary function $f(R)$. This extension introduces additional dynamical degrees of freedom capable of driving late-time acceleration and, in appropriate regimes, reproducing phenomena typically ascribed to dark matter. Within this class, power-law $f(R)$ models have been extensively studied for their success in explaining galactic rotation curves and gravitational lensing without requiring non-baryonic dark matter [40−42]. This idea has been further extended within broader geometric frameworks, including $f(T)$ gravity [43] based on torsion and $f(Q)$ gravity [44] grounded in nonmetricity, which provide distinct but dynamically equivalent avenues for explaining cosmic acceleration through modified spacetime geometry.

Beyond these frameworks, another widely studied possibility is an interaction between the dark sectors. In such scenarios, the exchange of energy and momentum between dark matter (DM) and dark energy (DE) gives rise to a broad class of models known as interacting dark energy (IDE) models [45−47]. In these constructions, the dark components are no longer independently conserved but are coupled through an interaction term, leading to modifications in both the background cosmic expansion and the evolution of linear perturbations. Dark photons provide complementary laboratory constraints on dark-sector interactions at electron–positron colliders [48]. In this work, we investigate the observational viability of a coupled ϕCDM cosmological model in which dark energy and dark matter interact through the derivative coupling term $Q = 3\alpha\dot{\rho}_m$ [49−51]. Motivated by recent indications of dynamical dark energy from DESI analyses [11−13], we constrain the interacting scenario using the DESI DR2 BAO measurements in combination with compressed CMB likelihoods, cosmic chronometer data, and three independent Type Ia supernova compilations (Pantheon$^+$, DES-Dovekie, and Union3). In contrast to several earlier interacting dark energy studies based on older observational datasets [52−54], our analysis incorporates the latest measurements and compares the coupled ϕCDM and ΛCDM models using Bayesian evidence. We further examine how different SNe Ia datasets affect the inferred constraints on the interaction parameter and the dark-energy equation of state. This analysis allows us to assess the robustness of interacting dark energy signatures in light of current cosmological observations. Our paper is organized as follows. In Section II, we introduce the theoretical background and the underlying model equations. Section III presents the datasets and methodology, where we employ a Markov Chain Monte Carlo analysis using the publicly available DESI DR2 data. Section IV presents the results and concluding remarks.

CPC Accepted

II. COSMOLOGICAL FRAMEWORK AND INTERACTING DARK ENERGY MODEL

For a spatially homogeneous and isotropic spacetime, the Friedmann-Lemaître-Robertson-Walker (FLRW) metric provides a geometric realization of the cosmological principle. In spherical polar coordinates, the corresponding line element takes the form:

$$ds^2 = -dt^2 + a^2(t)\left[\frac{dr^2}{1-kr^2} + r^2\left(d\theta^2 + \sin^2\theta\, d\phi^2\right)\right], \quad (1)$$

where $a(t)$ is the scale factor, and the curvature index values $k = +1, 0, -1$ correspond to closed, spatially flat, and open universes, respectively.

The dynamics of spacetime are governed by the Einstein–Hilbert action,

$$S = \int \left(\frac{R}{2\kappa} + \mathcal{L}_m\right)\sqrt{-g}\, d^4x, \quad (2)$$

where R is the Ricci scalar, $\kappa = \frac{8\pi G}{c^4}$, $\mathcal{L}_m$ is the Lagrangian density associated with the matter sector, and g is the determinant of the spacetime metric tensor $g_{\mu\nu}$. Setting $c = 1$ and varying the action (2) with respect to the metric yields the Einstein field equations,

$$G_{\mu\nu} = R_{\mu\nu} - \frac{1}{2}Rg_{\mu\nu} = \kappa T_{\mu\nu}, \quad (3)$$

where $R_{\mu\nu}$ is the Ricci tensor, and $T_{\mu\nu}$ denotes the energy–momentum tensor of the cosmic fluid.

Applying the field equations (3) to the FLRW metric (2) yields the Friedmann equations. For a spatially flat universe ($k = 0$), these equations can be written as

$$\left(\frac{\dot{a}}{a}\right)^2 = \frac{8\pi G}{3}\sum\rho, \qquad \frac{\ddot{a}}{a} = -\frac{4\pi G}{3}\sum(\rho + 3P), \tag{4}$$

where ρ and P denote the total energy density and pressure, respectively, and the summation includes all cosmic components, such as dark matter and dark energy.

In the absence of interactions between different components, energy conservation yields the standard continuity equation,

$$\dot{\rho} = -3H(1+w)\rho, \tag{5}$$

where $H = \dot{a}/a$ is the Hubble parameter and $w = P/\rho$ denotes the equation-of-state parameter.

In the coupled ϕCDM framework, dark energy is modeled as a scalar field that exchanges energy with dark matter. This interaction is characterized by a coupling term Q, which leads to the modified conservation equations,

$$\dot{\rho}_\phi = -3H\rho_\phi(1+w_\phi) - Q, \tag{6}$$

$$\dot{\rho}_m = -3H\rho_m(1+w_m) + Q, \tag{7}$$

where ρ_ϕ and ρ_m are the energy densities of the scalar field and matter, respectively, and w_ϕ and w_m are the corresponding equation-of-state parameters.

In this work, we investigate the viability of dynamical dark energy within the coupled ϕCDM framework, in which dark energy exchanges energy with dark matter through a coupling term (Q). We adopt the following form for the coupling term [49, 50]

$$Q = 3\alpha\dot{\rho}_m, \tag{8}$$

where α is a dimensionless coupling parameter that determines the interaction strength.

Unlike the commonly used interaction forms proportional to $H\rho_m$, $H\rho_{DE}$, or $H\rho_\phi$, or their linear combinations [45–47], the coupling considered in this work is determined by the time derivative of the matter energy density, $\dot{\rho}_m$. Since the matter component dominates the intermediate stage of cosmic evolution and plays a fundamental role in the transition from a decelerating to an accelerating Universe, it is physically natural to relate the interaction to the evolution of the matter sector rather than to its instantaneous energy density. Motivated by this picture, we adopt (8) as the interaction term. For a comparative analysis, see [55], which provides a comprehensive overview of interaction choices. Interacting dark energy scenarios with different coupling prescriptions have been widely explored in the literature [45–47], although certain classes of interacting models may develop instabilities at the perturbation level, particularly during the early evolution of the Universe [56, 57]. In the present work, we restrict our analysis to the homogeneous cosmological background and do not consider perturbation dynamics. A complete perturbative stability analysis of the coupled ϕCDM scenario is left for future investigation.

For pressureless dust matter ($w_m = 0$), the continuity equation (7) reduces to

$$\dot{\rho}_m = -3H\rho_m + Q. \tag{9}$$

Substituting the interaction term given in (8) yields

$$\dot{\rho}_m = -3H\rho_m + 3\alpha\dot{\rho}_m, \tag{10}$$

which can be rearranged as,

$$(1-3\alpha)\dot{\rho}_m = -3H\rho_m. \tag{11}$$

Using the relation $H = \dot{a}/a$, the preceding equation becomes

$$\frac{\dot{\rho}_m}{\rho_m} = -\frac{3}{1-3\alpha}\frac{\dot{a}}{a} \tag{12}$$

Integrating both sides of Eq. (12) gives the following scaling behavior for the matter density [49].

$$\rho_m = \rho_m^0\left(\frac{a}{a_0}\right)^{-\frac{3}{1-3\alpha}}, \tag{13}$$

where ρ_m^0 denotes the present-day matter energy density. Similarly, solving Eq. (6) for a constant scalar-field equation-of-state parameter w_ϕ yields

$$\rho_\phi = \frac{3\alpha\rho_m^0}{(1-3\alpha)(1+w_\phi)-1}\times\left[\left(\frac{a}{a_0}\right)^{-\frac{3}{1-3\alpha}} - \left(\frac{a}{a_0}\right)^{-3(1+w_\phi)}\right] + \rho_\phi^0\left(\frac{a}{a_0}\right)^{-3(1+w_\phi)}. \tag{14}$$

By substituting Eqs. (13) and (14) into the Friedmann equation (4), the Hubble parameter can be expressed as

$$\left(\frac{\dot{a}}{a}\right)^2 = \frac{8\pi G}{3}\left[\frac{3\alpha\rho_m^0}{(1-3\alpha)(1+w_\phi)-1}\left(\frac{a}{a_0}\right)^{-\frac{3}{1-3\alpha}} + \rho_m^0\left(\frac{a}{a_0}\right)^{-\frac{3}{1-3\alpha}} + \left(\rho_\phi^0 - \frac{3\alpha\rho_m^0}{(1-3\alpha)(1+w_\phi)-1}\right)\left(\frac{a}{a_0}\right)^{-3(1+w_\phi)}\right] \tag{15}$$

CPC Accepted

Introducing Characteristic Time Scales

$$t_m^2 = \frac{1}{H_0^2\Omega_m^0}, \qquad t_\phi^2 = \frac{1}{H_0^2\Omega_\phi^0}, \tag{16}$$

where Ω_m^0 and Ω_ϕ^0 denote the present-day density parameters for matter and the scalar field, respectively. Dividing Eq. (15) by its present value, Eq. (4), and defining the dimensionless Hubble parameter,

$$E(a) \equiv \frac{H(a)}{H_0} \tag{17}$$

$$E^2(a) = \Omega_m^0\left[\left(1+\frac{3\alpha}{D}\right)\left(\frac{a}{a_0}\right)^{-\frac{3}{1-3\alpha}} - \frac{3\alpha}{D}\left(\frac{a}{a_0}\right)^{-3\left(\frac{D+1}{1-3\alpha}\right)}\right] + \Omega_\phi^0\left(\frac{a}{a_0}\right)^{-3\left(\frac{D+1}{1-3\alpha}\right)}. \tag{18}$$

where $D = (1-3\alpha)(1+w_\phi)-1$. The dimensionless Hubble parameter can be expressed as a function of redshift as follows:

$$E^2(z) = \Omega_m^0\left[\left(1+\frac{3\alpha}{D}\right)(1+z)^{\frac{3}{1-3\alpha}} - \frac{3\alpha}{D}(1+z)^{\frac{3(D+1)}{1-3\alpha}}\right] + \Omega_\phi^0(1+z)^{\frac{3(D+1)}{1-3\alpha}}. \tag{19}$$

III. DATASET AND METHODOLOGY

The constraints on the parameters of the coupled ϕCDM model are obtained using Bayesian inference. This is implemented with the Metropolis–Hastings Markov Chain Monte Carlo (MCMC) algorithm [58] in the cosmological inference code `SimpleMC`[1]. The convergence of the MCMC sampling is assessed using the Gelman–Rubin convergence diagnostic, which serves as the stopping criterion for the simulations. The MCMC chains are terminated once the condition $R-1<0.01$ is satisfied [59]. After convergence, the resulting chains are post-processed with the `GetDist` package[2] [60] to obtain the 1D marginalized posterior distributions and 2D marginalized confidence contours.

Model comparison between the coupled ϕCDM and ΛCDM models is performed using Bayesian evidence. The Bayesian evidence, $\ln\mathcal{Z}$, is computed with the `MCEvidence` package[3] [61, 62]. The Bayesian evidence $\mathcal{Z}$ is defined as the integral of the likelihood function over the parameter space, $\mathcal{Z} = \int_\Omega P(D\,|\,\boldsymbol{\theta},M)\,P(\boldsymbol{\theta}\,|\,M)\,P(M)\,d\boldsymbol{\theta}$, where $P(D\,|\,\boldsymbol{\theta},M)$ denotes the likelihood of the observational data D given the model parameters $\boldsymbol{\theta}$, $P(\boldsymbol{\theta}\,|\,M)$ represents the prior distribution of the parameters, $P(M)$ is the prior probability assigned to the model, and Ω corresponds to the allowed parameter domain. The relative preference between the two models is quantified using the Bayes factor, evaluated in logarithmic form as $\ln B = \ln\mathcal{Z}_{\phi\mathrm{CDM}} - \ln\mathcal{Z}_{\Lambda\mathrm{CDM}}$, where $\mathcal{Z}_{\phi\mathrm{CDM}}$ and $\mathcal{Z}_{\Lambda\mathrm{CDM}}$ denote the Bayesian evidence values associated with the coupled ϕCDM and ΛCDM models, respectively. A positive value of $\ln B$ indicates a preference for the coupled ϕCDM model, whereas a negative value favours the ΛCDM model.

The statistical significance of the model comparison is interpreted according to the Jeffreys scale [63, 64]. Within this framework, values of $|\ln B_{\phi\mathrm{CDM},\Lambda\mathrm{CDM}}|<1$ correspond to inconclusive evidence; $1\leqslant|\ln B_{\phi\mathrm{CDM},\Lambda\mathrm{CDM}}|<2.5$ indicates weak evidence; $2.5\leqslant|\ln B_{\phi\mathrm{CDM},\Lambda\mathrm{CDM}}|<5$ is classified as moderate evidence; $5\leqslant|\ln B_{\phi\mathrm{CDM},\Lambda\mathrm{CDM}}|<10$ signifies strong evidence; and $|\ln B_{\phi\mathrm{CDM},\Lambda\mathrm{CDM}}|\geqslant 10$ provides decisive evidence for the model selected by the sign of $\ln B$.

This analysis is conducted using several combinations of observational data from baryon acoustic oscillations, cosmic chronometers, Type Ia supernovae, and compressed cosmic microwave background likelihoods, which are described in detail below.

- **Cosmic Chronometer**: First, we use Cosmic Chronometer (CC) observations, which provide direct and largely model-independent measurements of the Hubble parameter $H(z)$ based on the differential age method. In our analysis, we adopt a compilation of 15 CC measurements spanning the redshift range $0.1791\leqslant z\leqslant 1.965$ [65−67]. The likelihood is evaluated using the public implementation provided in Moresco's GitLab repository[4], which incorporates the full covariance matrix of the data.
- **Baryon Acoustic Oscillations:** We use Baryon Acoustic Oscillation (BAO) measurements from the Dark Energy Spectroscopic Instrument (DESI) Data Release 2 (DR2) [68], extracted from multiple tracers, including the Bright Galaxy Sample (BGS), Luminous Red Galaxies (LRG1–3), Emission Line Galaxies (ELG1–2), Quasars (QSO), and the Lyman-α forest. These measurements cover seven redshift bins over the range $0.3\leqslant z\leqslant 2.33$. The DESI DR2 BAO information is incorporated through the compressed distance measures D_M/r_d, D_H/r_d, and D_V/r_d, where $D_H(z)=c/H(z)$ is the Hubble distance,

1) https://github.com/ja-vazquez/SimpleMC.git
2) https://github.com/cmbant/getdist.git
3) https://github.com/yabebalFantaye/MCEvidence.git
4) https://gitlab.com/mmoresco/CCcovariance

CPC Accepted

$D_M(z) = c\int_0^z dz'/H(z')$ is the transverse comoving distance, $D_V(z) = [zD_M^2(z)D_H(z)]^{1/3}$ is the isotropic distance, and r_d denotes the sound horizon at the baryon drag epoch.

• **Type Ia Supernovae:** We also use three Type Ia supernova (SNe Ia) samples. The first is the Pantheon$^+$ compilation [69, 70], which contains 1,701 light curves from 1,550 SNe Ia over the redshift range $0.001 \leqslant z \leqslant 2.26$. To mitigate systematic effects from peculiar velocities at very low redshifts, we exclude light curves with $z < 0.01$, yielding a final sample of 1,590 light curves. Second, we use the recalibrated DES-Dovekie SNe Ia sample [71], which consists of 1,820 photometric light curves from the Dark Energy Survey Supernova Program over a five-year period. This dataset spans $0.02 \leqslant z \leqslant 1.14$ and includes 1,623 SNe Ia discovered by DES and 197 low-redshift SNe from external surveys such as CfA and CSP [72−74]. The revised catalog shares 1,718 SNe Ia with the DES-SN5YR sample [75]. Finally, we use the Union3 compilation [76], which consists of 2,087 SNe Ia over $0.05 < z < 2.26$, with 1,363 objects overlapping with Pantheon$^+$. In all analyses, we marginalize over the absolute magnitude nuisance parameter $\mathcal{M}$ following Eqs. (A9)–(A12) of Ref. [77].

• **Compressed CMB likelihood:** Finally, we use the compressed CMB likelihood, defined by the parameter vector $\mathbf{v} = (\theta_s, \omega_b, \omega_{bc})$, and model it as a 3×3 multivariate Gaussian likelihood. Further details can be found in Appendix A of [68].

The chosen priors for the ΛCDM and coupled ϕCDM models are summarized in Table 1. We adopt the phenomenological prior $\alpha \in [-2, 2]$ and examine the sensitivity of the Bayesian evidence to the prior range by considering a narrower interval, $\alpha \in [-2, 0.29]$. For this alternative prior, we obtain log Bayes factors of $\ln B = -5.93$, -5.65, -5.39, and -5.03 for CMB + DESI DR2 + CC, CMB + DESI DR2 + CC + Pantheon$^+$, CMB + DESI DR2 + CC + DES-Dovekie, and CMB + DESI DR2 + CC + Union3, respectively. These values do not differ significantly from those obtained with the original prior $\alpha \in [-2, 2]$, as reported in Table 2, indicating that the Bayesian evidence and the resulting preference for ΛCDM remain largely unchanged. Thus, although Bayesian evidence is generally sensitive to the adopted prior volume, our model-comparison conclusions are robust within the examined prior ranges.

Table 1. The table summarizes the priors adopted in our analysis of the ΛCDM and coupled ϕCDM models. Here, $\mathcal{U}$ denotes a uniform prior, and $h \equiv H_0/100$.

Model	Parameter	Prior
ΛCDM	Ω_{m0} (default)	$\mathcal{U}[0, 1]$
	$h = H_0/100$ (default)	$\mathcal{U}[0, 1]$
Coupled ϕCDM	α	$\mathcal{U}[-2.0, 2.0]$
	w_ϕ	$\mathcal{U}[-3.0, 1.0]$
	Ω_{m0}, h (default)	see above

IV. RESULTS AND DISCUSSIONS

Fig. 1 shows the joint and marginalized posterior distributions of the cosmological parameters of the coupled ϕCDM model obtained from the MCMC analysis. The contours represent the 1σ and 2σ confidence regions, while the diagonal panels show the corresponding one-dimensional (1D) marginalized distributions. The off-diagonal panels display the two-dimensional (2D) posterior distributions for each parameter pair, illustrating the correlations between parameters for different dataset combinations. The posterior distributions obtained from the four dataset combinations show substantial overlap, indicating that the estimated cosmological parameters remain largely insensitive to the choice of the SNe Ia compilation. Although the inclusion of the Pantheon$^+$, DES-Dovekie, and Union3 datasets leads to slightly tighter confidence regions than those obtained from the CMB+DESI DR2+CC dataset alone, no noticeable shift in the best-fit parameter values is observed. In addition, the interaction parameter α is well constrained within a narrow range, implying that current observational data are consistent with only a weak interaction between dark energy and dark matter.

Table 2 presents the mean values and corresponding 68% (1σ) confidence intervals for the ΛCDM and coupled ϕCDM models obtained using different combinations of the CMB, DESI DR2, CC, and SNe Ia datasets. For the ΛCDM model, the inferred values of the dimensionless Hubble parameter lie in the range $h \simeq 0.679$–0.682, whereas the coupled ϕCDM model predicts slightly higher values, with $h \simeq 0.680$–0.690.

To quantify the level of agreement with the local determination of the Hubble constant, we compare our results with the SH0ES measurement, $h = 0.730 \pm 0.010$ [78]. For the CMB + DESI DR2 + CC dataset, the tension is reduced from 4.46σ in the ΛCDM model to 2.69σ in the coupled ϕCDM model. After including the Pantheon$^+$ sample, the tension changes from 4.65σ to 3.77σ. For the CMB + DESI DR2 + CC + DES-Dovekie combination, the tension decreases from 4.74σ to 3.85σ, while for CMB + DESI DR2 + CC + Union3, it is reduced from 4.56σ to 3.90σ. These results show that the coupled ϕCDM model consistently shifts the inferred value of H_0 toward the SH0ES measurement, thereby reducing the tension relative to the ΛCDM model. Nevertheless, the remaining discrepancy remains statistically significant, indicating that the model does not provide a complete resolution of the H_0 tension. This behaviour is also illustrated in Fig. 2.

CPC Accepted

Table 2. This table presents the mean values and corresponding uncertainties at the 68% (1σ) confidence level for the ΛCDM and coupled ϕCDM models, obtained from DESI DR2 and cosmic chronometer (CC) measurements combined with the compressed CMB likelihood and three different SNe Ia samples (Pantheon$^+$, DES-Dovekie, and Union3).

Parameter	Dataset	ΛCDM Model	Coupled ϕCDM Model
h	CMB + DESI DR2 + CC	0.682 ± 0.004	0.690 ± 0.011
	CMB + DESI DR2 + CC + Pantheon$^+$	$0.679^{+0.005}_{-0.004}$	0.684 ± 0.007
	CMB + DESI DR2 + CC + DES-Dovekie	0.679 ± 0.004	0.683 ± 0.007
	CMB + DESI DR2 + CC + Union3	0.679 ± 0.005	0.680 ± 0.008
Ω_m	CMB + DESI DR2 + CC	0.303 ± 0.005	0.301 ± 0.009
	CMB + DESI DR2 + CC + Pantheon$^+$	0.306 ± 0.006	0.305 ± 0.006
	CMB + DESI DR2 + CC + DES-Dovekie	0.307 ± 0.005	0.306 ± 0.006
	CMB + DESI DR2 + CC + Union3	0.306 ± 0.006	0.308 ± 0.007
α	CMB + DESI DR2 + CC	—	-0.00045 ± 0.00048
	CMB + DESI DR2 + CC + Pantheon$^+$	—	-0.00054 ± 0.00047
	CMB + DESI DR2 + CC + DES-Dovekie	—	-0.00057 ± 0.00048
	CMB + DESI DR2 + CC + Union3	—	-0.00061 ± 0.00048
w_ϕ	CMB + DESI DR2 + CC	—	-0.980 ± 0.044
	CMB + DESI DR2 + CC + Pantheon$^+$	—	-0.954 ± 0.027
	CMB + DESI DR2 + CC + DES-Dovekie	—	-0.951 ± 0.026
	CMB + DESI DR2 + CC + Union3	—	-0.939 ± 0.033
$\ln \mathcal{B}_{\phi\text{CDM},\Lambda\text{CDM}}$	CMB + DESI DR2 + CC	0	−5.94
	CMB + DESI DR2 + CC + Pantheon$^+$	0	−5.66
	CMB + DESI DR2 + CC + DES-Dovekie	0	−5.42
	CMB + DESI DR2 + CC + Union3	0	−5.10

CPC Accepted

We now compare the constraints on the present-day matter density parameter, Ω_m, for the ΛCDM and coupled ϕCDM models. For the ΛCDM model, the inferred values lie in the range $\Omega_{m0} \simeq 0.303$–0.307 across the different combinations of the CMB, DESI DR2, CC, and SNe Ia datasets. The coupled ϕCDM model yields very similar constraints, with $\Omega_{m0} \simeq 0.301$–0.308. For the CMB + DESI DR2 + CC dataset, the coupled ϕCDM model gives a slightly lower value, $\Omega_{m0} = 0.301 \pm 0.009$, compared with $\Omega_{m0} = 0.303 \pm 0.005$ in the ΛCDM model. After including the Pantheon$^+$ and DES-Dovekie supernova samples, both models provide nearly identical constraints, with differences well within the 1σ uncertainties. For the Union3 dataset, the coupled ϕCDM model yields a marginally higher value, $\Omega_{m0} = 0.308 \pm 0.007$, compared with $\Omega_{m0} = 0.306 \pm 0.006$ in the ΛCDM model. Overall, the constraints on the present-day matter density parameter remain consistent between the two cosmological models, indicating that the introduction of the coupling has only a negligible impact on the determination of Ω_m.

Turning to the interaction parameter α, which characterizes the energy exchange between dark matter and dark energy, we note that its sign determines the direction of energy transfer: negative values correspond to energy flow from dark energy to dark matter, whereas positive values indicate the opposite direction. As shown in Table 2, this parameter is consistently constrained to small negative values for all dataset combinations, with $\alpha = -0.00045 \pm 0.00048$ for CMB + DESI DR2 + CC, $\alpha = -0.00054 \pm 0.00047$ after including Pantheon$^+$, $\alpha = -0.00057 \pm 0.00048$ with DES-Dovekie, and $\alpha = -0.00061 \pm 0.00048$ when the Union3 sample is added. In all cases, the constraints are consistent with $\alpha = 0$ within the 1σ confidence level. Therefore, although the best-fit values show a mild preference for a negative interaction, corresponding to energy transfer from dark energy to dark matter, the current data do not provide statistically significant evidence for a non-zero interaction between the two dark sectors.

Interestingly, the preferred late-time direction of energy transfer inferred from our analysis is qualitatively consistent with the recent results of Zhang *et al.* [79], who analyzed an interacting ξ-index dark-energy model using DESI 2025 BAO, Pantheon$^+$, Planck, and ACT observations. They similarly reported a preference for a negative interaction, corresponding to a net energy flow from dark energy to the matter sector, although the current observational evidence was found to be statistically

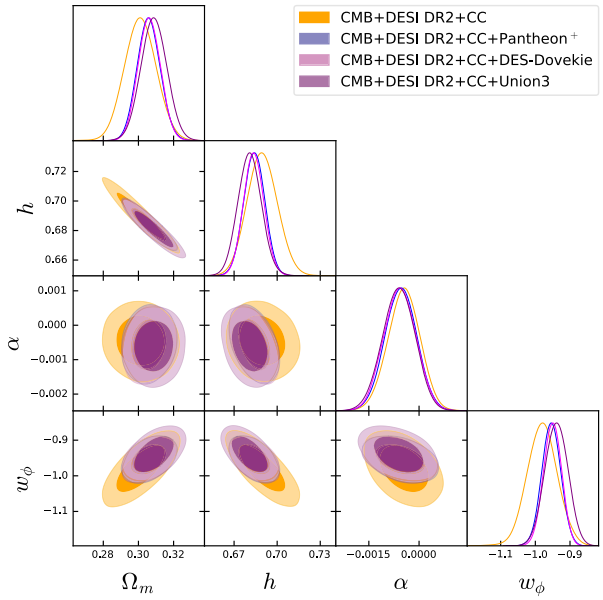


Fig. 1. (color online) The figure presents the corner plot for the coupled ϕCDM model at the 68% (1σ) and 95% (2σ) confidence levels, using DESI DR2 and cosmic chronometer (CC) data combined with a compressed CMB likelihood and different SNe Ia samples (Pantheon$^+$, DES-Dovekie, and Union3).

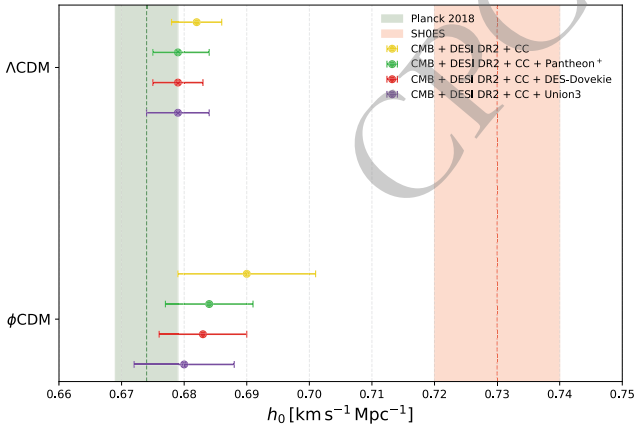


Fig. 2. (color online) Comparison of the inferred values of h_0 for the ΛCDM and coupled ϕCDM models from CMB+DESI DR2+CC alone and in combination with the Pantheon+, DES-Dovekie, and Union3 supernova samples.

inconclusive. We emphasize that this agreement concerns only the preferred direction of late-time energy transfer. The interaction mechanisms differ, since the present work adopts the derivative coupling $Q = 3\alpha\dot{\rho}_m$, whereas Ref. [79] considers an interacting ξ-index dark-energy model.

The constraints on the dark energy equation-of-state parameter w_ϕ favour values greater than -1 across all dataset combinations, corresponding to a quintessence-like dark energy scenario. We find $w_\phi = -0.980 \pm 0.044$ for CMB + DESI DR2 + CC, corresponding to a deviation of approximately 0.45σ from the cosmological constant value, $w = -1$. After including the Pantheon$^+$ sample, the constraint becomes $w_\phi = -0.954 \pm 0.027$, corresponding to a 1.70σ deviation. For the CMB + DESI DR2 + CC + DES-Dovekie combination, we obtain $w_\phi = -0.951 \pm 0.026$, corresponding to a 1.88σ deviation, while the CMB + DESI DR2 + CC + Union3 dataset yields $w_\phi = -0.939 \pm 0.033$, corresponding to a 1.85σ deviation. Although the mean values consistently favour the quintessence regime ($w_\phi > -1$), all measurements remain compatible with $w = -1$ within the 2σ confidence level.

Using the logarithmic Bayes factor, we statistically compare the coupled ϕCDM model with ΛCDM. We find $\ln B_{\phi\mathrm{CDM},\Lambda\mathrm{CDM}} = -5.94$, -5.66, -5.42, and -5.10 for the CMB + DESI DR2 + CC, CMB + DESI DR2 + Pantheon$^+$ + CC, CMB + DESI DR2 + DES-Dovekie + CC, and CMB + DESI DR2 + Union3 + CC dataset combinations, respectively. The negative values indicate a strong preference for the ΛCDM model over the coupled ϕCDM model, according to the Jeffreys scale.

A. Limitations and Future Scope

The present analysis is restricted to the homogeneous background evolution of the coupled ϕCDM model using background cosmological observations, including DESI DR2 BAO, compressed CMB likelihoods, and Type Ia supernova data. Although the adopted interaction successfully describes the background expansion history, several important aspects remain beyond the scope of this work.

First, the analysis does not include the evolution of cosmological perturbations or the corresponding growth of large-scale structure. Consequently, the perturbative stability of the interaction term $Q = 3\alpha\dot{\rho}_m$ has not been investigated. Second, the interaction parameter α and the equation-of-state parameter w_ϕ have been assumed to remain constant throughout cosmic evolution. More general scenarios involving time-dependent interactions and dynamical equations of state may provide additional physical insight. Third, the present analysis employs compressed CMB likelihoods rather than the full CMB likelihood. Although the compressed likelihood provides robust constraints on the background expansion history, it does not fully exploit the information contained in the CMB temperature and polarization anisotropies. A full CMB likelihood analysis requires the dedicated implementation and validation of the coupled ϕCDM model within a Boltzmann solver and is therefore beyond the scope of the present work.

Future studies incorporating the full CMB likelihood, redshift-space distortion measurements, weak-lensing observations, and forthcoming high-precision surveys such as Euclid and the Roman Space Telescope will enable a

CPC Accepted

more comprehensive assessment of coupled dark energy models and their perturbation-level predictions. These extensions constitute promising directions for future work and may further clarify whether any statistically significant dark-sector interaction exists beyond current observational limits.

V. CONCLUSIONS

In this work, we have investigated observational constraints at the background level on the coupled ϕCDM cosmological model using DESI DR2 BAO measurements, compressed CMB likelihoods, and various Type Ia supernova datasets. The analysis focused on constraining the model parameters and assessing the model's performance relative to the standard ΛCDM model through Bayesian model comparison. The key findings of this study are summarized below:

• We constrained the coupled ϕCDM model using combinations of CMB, DESI DR2, Pantheon$^+$, DES-Dovekie, and Union3 datasets and compared its performance with that of the standard ΛCDM model.

• The coupled ϕCDM model yields background-level cosmological constraints that are broadly consistent with those of ΛCDM. Although it produces a slight shift toward higher H_0 values, this shift is insufficient to resolve the Hubble tension.

• The present-day matter density parameter Ω_m^0 remains tightly constrained and shows no significant deviation from the value preferred by the standard cosmological model.

• The interaction parameter α shows a slight preference for negative values, suggesting a possible energy transfer from dark energy to dark matter. This preferred direction is qualitatively consistent with recent studies of interacting dark energy that report a late-time energy flow from dark energy to the matter sector [79]. However, $\alpha = 0$ remains consistent within the 1σ confidence level, indicating no statistically significant evidence for a dark-sector interaction.

• The dark energy equation-of-state parameter w_ϕ remains close to -1, exhibiting only marginal deviations toward quintessence-like behavior.

• Bayesian model comparison consistently favors the ΛCDM model over the coupled ϕCDM scenario across all dataset combinations. On the Jeffreys scale, this preference ranges from moderate to strong.

• Although there is no significant evidence for coupling, the mild trends observed in w_ϕ and α, together with recent indications of dynamical dark energy from DESI analyses, motivate further investigation of interacting dark-energy models using future high-precision cosmological observations.

• The present analysis is limited to the homogeneous background cosmological evolution with constant interaction and equation-of-state parameters. Future work will incorporate cosmological perturbations, structure-formation observations, the full CMB likelihood, and more general scenarios involving time-dependent interactions. This will enable a more rigorous assessment of the coupled ϕCDM model and its observational viability.

CPC Accepted

ACKNOWLEDGEMENT

We thank the anonymous reviewers for their insightful comments and constructive suggestions, which improved the quality and clarity of this manuscript. S. D. Pathak acknowledges the Inter-University Centre for Astronomy and Astrophysics (IUCAA), Pune, where this work was carried out under its 'Associate Programme'. Sahit Kumar is grateful to Vipin Kumar Sharma for useful discussions and valuable comments. S. D. Pathak also expresses his gratitude to all those whose dedication and often unnoticed contributions to the pursuit of science and knowledge advance scientific research.

References

[1] A. G. Riess, A. V. Filippenko, P. Challis, A. Clocchiatti, A. Diercks, P. M. Garnavich, R. L. Gilliland, C. J. Hogan, S. Jha, R. P. Kirshner, *et al.*, The astronomical journal **116**(3), 1009 (1998)

[2] S. Perlmutter, G. Aldering, G. Goldhaber, R. A. Knop, P. Nugent, P. G. Castro, S. Deustua, S. Fabbro, A. Goobar, D. E. Groom, *et al.*, The Astrophysical Journal **517**(2), 565 (1999)

[3] P. A. Ade, N. Aghanim, C. Armitage-Caplan, M. Arnaud, M. Ashdown, F. Atrio-Barandela, J. Aumont, C. Baccigalupi, A. J. Banday, R. Barreiro, *et al.*, Astronomy & Astrophysics **571**, A16 (2014)

[4] N. Aghanim, Y. Akrami, F. Arroja, M. Ashdown, J. Aumont, C. Baccigalupi, M. Ballardini, A. J. Banday, R. Barreiro, N. Bartolo, *et al.*, Astronomy & Astrophysics **641**, A1 (2020)

[5] N. Aghanim, *et al.*, Astron. Astrophys **641**, A6 (2020)

[6] T. Padmanabhan, Phys. Rept. **380**, 235 (2003)

[7] E. J. Copeland, M. Sami, S. Tsujikawa, International Journal of Modern Physics D **15**(11), 1753 (2006)

[8] S. Weinberg, Reviews of modern physics **61**(1), 1 (1989)

[9] S. M. Carroll, Living Rev. Rel. **4**, 1 (2001)

[10] I. Zlatev, L.-M. Wang, P. J. Steinhardt, Quintessence, cosmic coincidence, Phys. Rev. Lett. **82**, 896 (1999)

[11] A. Adame, *et al.*, Journal of Cosmology and Astroparticle Physics **2025**(02), 021 (2025)

[12] M. Abdul-Karim, J. Aguilar, S. Ahlen, S. Alam, L. Allen, C. A. Prieto, O. Alves, A. Anand, U. Andrade, E. Armengaud, *et al.*, Desi dr2 results ii: Measurements of baryon acoustic oscillations and cosmological constraints, arXiv preprint arXiv: 2503.14738 (2025).

[13] K. Lodha, *et al.*, Phys. Rev. D **112**(8), 083511 (2025)

[14] H. Chaudhary, V. K. Sharma, S. Capozziello, G. Mustafa, Astrophys. J. Suppl. **283**(2), 73 (2026)
[15] V. K. Sharma, H. Chaudhary, S. Kolekar, Journal of High Energy Astrophysics 100518 (2025)
[16] H. Chaudhary, S. Capozziello, V. K. Sharma, G. Mustafa, The Astrophysical Journal **992**(2), 194 (2025)
[17] H. Chaudhary, S. Capozziello, V. K. Sharma, I. Gómez-Vargas, G. Mustafa, DES-Dovekie, and Union3, Eur. Phys. J. C **86**(5), 564 (2026)
[18] H. Chaudhary, S. Capozziello, S. Praharaj, S. K. J. Pacif, G. Mustafa, Journal of High Energy Astrophysics 100507 (2025)
[19] H. Chaudhary, V. K. Sharma, S. Capozziello, G. Mustafa, The Astrophysical Journal Supplement Series **283**(2), 73 (2026)
[20] S. Capozziello, H. Chaudhary, T. Harko, G. Mustafa, Physics of the Dark Universe 102196 (2025)
[21] H. Chaudhary, R. Mandal, M. Bashir, V. K. Sharma, U. Debnath, Chin. Phys. C **50**, 045103 (2026)
[22] A. Kandel, F. Atamurotov, E. Güdekli, P. Channuie, G. Rakhimova, Eur. Phys. J. C **86**(7), 762 (2026)
[23] S. Capozziello, H. Chaudhary, G. Mustafa, S. K. J. Pacif, Astron. Astrophys. **709**, A258 (2026)
[24] H. Chaudhary, R. Nagpal, S. Pacif, G. Mustafa, The Astrophysical Journal Supplement Series **278**(1), 22 (2025)
[25] R. Nagpal, H. Chaudhary, H. Gupta, S. Pacif, Journal of High Energy Astrophysics **47**, 100396 (2025)
[26] V. Kumar Sharma, H. Chaudhary, S. Capozziello, J. Gogoi Dhruba, G. Mustafa, Phys. Dark Univ. **53**, 102383 (2026)
[27] V. Kumar Sharma, R. Kumar, H. Chaudhary, F. Atamurotov, JHEAp **53**, 100644 (2026)
[28] A. Mehrotra, H. Chaudhary, S. Pacif, International Journal of Geometric Methods in Modern Physics 2650092 (2025)
[29] B. Ratra, P. J. Peebles, Physical Review D **37**(12), 3406 (1988)
[30] R. R. Caldwell, R. Dave, P. J. Steinhardt, Physical Review Letters **80**(8), 1582 (1998)
[31] S. Kumar, S. D. Pathak, M. Khlopov, International Journal of Theoretical Physics **63**(9), 238 (2024)
[32] J. Kaur, S. D. Pathak, M. Khlopov, M. Krasnov, M. Sharma, Nuclear Physics B **1018**, 117010 (2025)
[33] J. Kaur, S. D. Pathak, V. K. Ojha, M. Y. Khlopov, Astroparticle Physics **157**, 102926 (2024)
[34] R. R. Caldwell, Physics Letters B **545**(1-2), 23 (2002)
[35] A. Sen, Mod. Phys. Lett. A **17**, 1797 (2002)
[36] J. Kaur, S. D. Pathak, M. Khlopov, M. Sharma, Universe **11**(4), 131 (2025)
[37] B. Feng, The quintom model of dark energy, arXiv preprint astro-ph/0602156 (2006).
[38] W. Hu, I. Sawicki, Phys. Rev. D **76**, 064004 (2007)
[39] S. Capozziello, M. De Laurentis, Physics Reports **509**(4-5), 167 (2011)
[40] V. Kumar Sharma, M. M. Verma, Eur. Phys. J. C **82**(5), 400 (2022)
[41] V. K. Sharma, B. K. Yadav, M. M. Verma, The European Physical Journal C **81**(2), 109 (2021)
[42] V. K. Sharma, B. K. Yadav, M. M. Verma, The European Physical Journal C **80**(7), 619 (2020)
[43] G. R. Bengochea, R. Ferraro, Phys. Rev. D **79**, 124019 (2009)
[44] J. Beltrán Jiménez, L. Heisenberg, T. Koivisto, Phys. Rev. D **98**(4), 044048 (2018)
[45] B. Wang, E. Abdalla, F. Atrio-Barandela, D. Pavón, Rept. Prog. Phys. **87**(3), 036901 (2024)
[46] D. Figueruelo, M. van der Westhuizen, A. Abebe, E. Di Valentino, Phys. Dark Univ. **52**, 102238 (2026)
[47] R. Nagpal, A. Kandel, R. Mandal, U. Debnath, S. K. J. Pacif, SSFDE Model: Cosmological Implications and Dynamical System Analysis (11 2025). arXiv: 2511.06129.
[48] J. Jiang, C. Y. Li, S. Y. Li, S. D. Pathak, Z. G. Si, X. H. Yang, Chinese Phys. C **44**(2), 023105 (2020)
[49] M. M. Verma, S. D. Pathak, International Journal of Theoretical Physics **51**(8), 2370 (2012)
[50] M. Shahalam, S. D. Pathak, S. Li, R. Myrzakulov, A. Wang, The European Physical Journal C **77**(10), 686 (2017)
[51] S. Kumar, S. D. Pathak, X. Zhang, Europhysics Letters **150**(2), 29001 (2025)
[52] W. Yang, L. Xu, Phys. Rev. D **89**(8), 083517 (2014)
[53] T.-N. Li, P.-J. Wu, G.-H. Du, S.-J. Jin, H.-L. Li, J.-F. Zhang, X. Zhang, Astrophys. J. **976**(1), 1 (2024)
[54] D. Benisty, S. Pan, D. Staicova, E. Di Valentino, R. C. Nunes, Astron. Astrophys. **688**, A156 (2024)
[55] B. Wang, E. Abdalla, F. Atrio-Barandela, D. Pavón, Reports on Progress in Physics **79**, 096901 (2016)
[56] M. B. G. *et al*., JCAP **07**, 034 (2009)
[57] J. Valiviita, E. Majerotto, R. Maartens, JCAP **07**, 020 (2008)
[58] W. K. Hastings, Monte carlo sampling methods using markov chains and their applications (1970).
[59] A. Gelman, D. B. Rubin, Statistical science **7**(4), 457 (1992)
[60] A. Lewis, Journal of Cosmology and Astroparticle Physics **2025**(08), 025 (2025)
[61] A. Heavens, Y. Fantaye, E. Sellentin, H. Eggers, Z. Hosenie, S. Kroon, A. Mootoovaloo, Physical review letters **119**(10), 101301 (2017)
[62] A. Heavens, Y. Fantaye, A. Mootoovaloo, H. Eggers, Z. Hosenie, S. Kroon, E. Sellentin, Marginal likelihoods from monte carlo markov chains, arXiv preprint arXiv: 1704.03472 (2017).
[63] R. E. Kass, A. E. Raftery, Bayes factors, Journal of the american statistical association 90 (430) (1995) 773–795.
[64] R. Trotta, Contemporary Physics **49**(2), 71 (2008)
[65] M. Moresco, A. Cimatti, R. Jimenez, L. Pozzetti, G. Zamorani, M. Bolzonella, J. Dunlop, F. Lamareille, M. Mignoli, H. Pearce, *et al*., 2012 (08), 006 (2012)
[66] M. Moresco, Letters **450**(1), L16 (2015)
[67] M. Moresco, L. Pozzetti, A. Cimatti, R. Jimenez, C. Maraston, L. Verde, D. Thomas, A. Citro, R. Tojeiro, D. Wilkinson, Journal of Cosmology and Astroparticle Physics **2016**(05), 014 (2016)
[68] M. A. Karim, J. Aguilar, S. Ahlen, S. Alam, L. Allen, C. A. Prieto, O. Alves, A. Anand, U. Andrade, E. Armengaud, *et al*., Desi dr2 results. ii. measurements of baryon acoustic oscillations and cosmological constraints, Physical Review D 112 (8) (2025).
[69] D. Scolnic, D. Brout, A. Carr, A. G. Riess, T. M. Davis, A. Dwomoh, D. O. Jones, N. Ali, P. Charvu, R. Chen, *et al*., The Astrophysical Journal **938**(2), 113 (2022)
[70] D. Brout, D. Scolnic, B. Popovic, A. G. Riess, A. Carr, J. Zuntz, R. Kessler, T. M. Davis, S. Hinton, D. Jones, *et al*., The Astrophysical Journal **938**(2), 110 (2022)
[71] B. Popovic, P. Shah, W. Kenworthy, R. Kessler, T. Davis, A. Goobar, D. Scolnic, M. Vincenzi, P. Wiseman, R. Chen, *et al*., The dark energy survey supernova program: A

CPC Accepted

reanalysis of cosmology results and evidence for evolving dark energy with an updated type ia supernova calibration, arXiv preprint arXiv: 2511.07517 (2025).
[72] M. Hicken, P. Challis, S. Jha, R. P. Kirshner, T. Matheson, M. Modjaz, A. Rest, W. M. Wood-Vasey, G. Bakos, E. J. Barton, *et al*., The Astrophysical Journal **700**(1), 331 (2009)
[73] M. Hicken, P. Challis, R. P. Kirshner, A. Rest, C. E. Cramer, W. M. Wood-Vasey, G. Bakos, P. Berlind, W. R. Brown, N. Caldwell, *et al*., The Astrophysical Journal Supplement Series **200**(2), 12 (2012)
[74] R. Foley, Keck Observatory Archive **U079**, 39 (2017)
[75] T. Abbott, M. Acevedo, M. Aguena, A. Alarcon, S. Allam, O. Alves, A. Amon, F. Andrade-Oliveira, J. Annis, P. Armstrong, *et al*., The dark energy survey: Cosmology results with~ 1500 new high-redshift type ia supernovae using the full 5-year dataset, arXiv preprint arXiv: 2401.02929 (2024).
[76] D. Rubin, G. Aldering, M. Betoule, A. Fruchter, X. Huang, A. G. Kim, C. Lidman, E. Linder, S. Perlmutter, P. Ruiz-Lapuente, *et al*., The Astrophysical Journal **986**(2), 231 (2025)
[77] M. Goliath, R. Amanullah, P. Astier, A. Goobar, R. Pain, Astronomy & Astrophysics **380**(1), 6 (2001)
[78] A. G. Riess, *et al*., Astrophys. J. Lett. **934**(1), L7 (2022)
[79] Z. Zhang, T. Xu, Y. Chen, Astrophys. J. **999**(2), 248 (2026), arXiv: 2512.07281

CPC Accepted